

PHOTONIC-CRYSTAL FIBERS GYROSCOPES**1. Introduction**

Fiber optic gyroscopes (FOG) are generally recognized as promising for the control and navigation systems moving objects of various kinds (ground transportation, ships, aircraft, etc.). At the same time demand are (fiber optical gyroscope) in a wide range of characteristics of accuracy – 10.0 deg/h to 0, 001 deg / hr. In Russia, the leader in the production of a number of FOG accuracy class 10.0-1.0 deg/h is LLC "Physoptic". However, there is a gap from the foreign generally recognized as FOG for the control and navigation systems moving objects of various kinds level in FOG navigational accuracy class (0.01–0.001 deg/h). Performance characteristics of fiber-optic gyroscope increased accuracy are largely dependent on the characteristics of its basic elements and features of its assembly techniques. Thus, the development of fiber-optic gyroscope and methods of its production is an urgent task. Due to their unique geometric structure, photonic crystal fibers present special properties and capabilities that lead to an outstanding potential for sensing applications. The diversity of unusual features of photonic crystal fibers, beyond what conventional fibers can offer, leads to an increase of possibilities for new and improved sensors. There is a huge interest of the scientific community in this original technology for applications in a variety of fields. The aim of this work was to conduct theoretical studies of the conditions of photonic crystal fiber (PCF) usage as a part of the fiber optical gyroscope. Photonic crystal fiber gyroscopes are a kind of optics gyroscopes that present a diversity of new and improved features beyond what conventional optical fiber gyroscopes can offer.

2. The purpose and the goals of the paper

The main aim of this paper is using photonic crystal fiber as part of the gyroscopes because there are many reasons as shown below

A wide variety of fiber-optic-based sensing schemes have been proposed and reported to date, such schemes have a number of disadvantages such as high coupling losses, limited mechanical reliability, and difficulties in mass production. Photonic crystal fibers should present properties such as small size, simple design, and an all-fiber configuration with high measurement accuracy.

Photonic crystal fibers are used because unlike their conventional counterparts, Photonic crystal fiber-based sensing techniques minimally disturb the electric or magnetic field, and apart from the sensor head, the connecting fibers are inherently immune to electromagnetic interference. Also, they can provide true dielectric isolation between the sensor and the interrogation system in the presence of very high electromagnetic fields.

According to these features we can elimination a lot of the problems that exist in the conventional fiber optic gyroscope and getting better and more accurate results in the same conditions when using Photonic Crystal Fibers.

3. Sagnac Interferometer optical fibers

Sagnac interferometers (SIs) are recently in great interest in various sensing applications owing to their advantages of simple structure, easy fabrication, and environmental robustness [1]. SI consists of an optical fiber loop, along which two beams are propagating in counter directions with different polarization states. As schematically illustrated in Fig. 1, the input light is split into two directions by a 3dB fiber coupler and the two counter-propagating beams are combined again at the same coupler. Unlike other fiber optic interferometers, the OPD is determined by the polarization dependent propagating speed of the mode guided along the loop. To maximize the polarization-dependent feature of SIs, birefringent fibers are typically utilized in sensing parts. The polarizations are adjusted by a polarization controller (PC) attached at the beginning of the sensing fiber. The

signal at the output port of the fiber coupler is governed by the interference between the beams polarized along the slow axis and the fast axis. The phase of the interference is simply given as:

$$d = \frac{2p}{l} BL, \quad (1)$$

$$B = |n_f - n_s|.$$

Where B is the birefringent coefficient of the sensing fiber, L is the length of the sensing fiber, and n_f and n_s are the effective indices of the fast and slow modes, respectively [1].

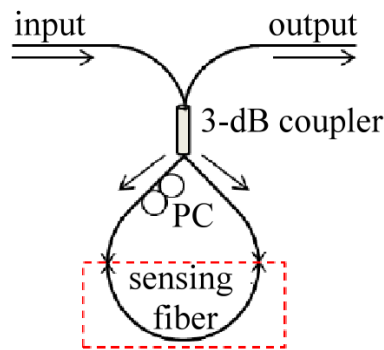


Fig. 1. Sensor based on a Sagnac interferometer

Fig. 1 is schematic of the sensor based on a Sagnac interferometer. In general, high birefringent fibers (HBFs) or polarization maintaining fibers (PMFs) are chosen as the sensing fibers to acquire high phase sensitivity.

4. Principles of work of fiber optic gyroscope

Fiber optical gyroscope is based on the Sagnac effect [2]. Sagnac effect generates an optical phase difference, $\Delta\phi$, between two counter propagating waves in a rotating fiber coil (optical path)[3]:

$$Dj = \frac{8pS}{lc} W, \quad (2)$$

where ($\Delta\phi$) – phase difference, Ω – angular velocity, C – light /signal velocity, λ – wavelength, S – scale factor

Fig. 2 open-loop (FOG) is scheme of fiber optic gyroscope . They are widely used in commercial applications where their dynamic range and linearity limitations are not constraining.

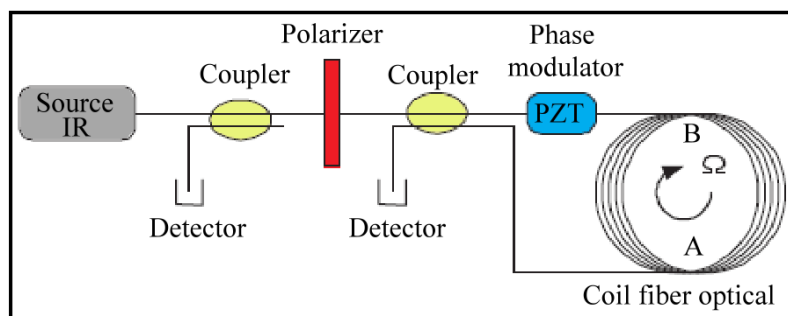


Fig. 2. Scheme of fiber optic gyroscope

However, a clear and precise definition of the angular velocity is necessary to exclude the possibility of additive and multiplicative effects of other physical effects on the measured value of the phase difference of counter propagating waves. The main challenge to the realization of high-precision phase measurements is a zero drift, which is manifested in the fact that physically station-

ary gyroscope output signal there, which is due to physical phenomena not related to the rotation of the loop. In the fiber material in a medium to obtain a stable optical phase oscillations is practically impossible. Therefore fiber optic gyroscopes may occur an additive phase noise. One of the reasons for the appearance of these signals is the scattering and reflection in a fiber loop. During the rotation angular velocity contour (Ω), an apparent distance between points A and B for the oppositely traveling beams changes. For a wave traveling from point A to point B, i.e., in direction similar to the direction of rotation of the contour, the distance is extended, as in a time dt point B moves to the angle ($d\phi = \Omega \cdot dt$). This is for lengthening the path of the light beam is equal to dt , since at each instant the beam is directed at a tangent to the contour at that same tangential linear velocity directed projection ($\bar{u} = \bar{u} \cdot \cos a = \Omega r \cdot \cos a$). Thus, the length of the path traversed by the beam is equal to $dl + \bar{u} \cdot dt$. Arguing similarly, for opposing traveling light beam will be a reduction in the apparent path segment $dl - \bar{u} \cdot dt$. Considering the speed of light invariant quantity, apparent elongation and reduction paths for opposing beams can be considered equivalent to extensions and contractions of time intervals, i.e.,

$$Dt_1 = \frac{1}{c}(dl + n \cdot dt) \quad (3)$$

$$Dt_2 = \frac{1}{c}(dl - n \cdot dt) \quad (4)$$

If the relative time delay of counter propagating waves occurring during the rotation, expressed in terms of the phase difference of counters propagating waves, it will be

$$Dj = \omega \cdot Dt = \frac{4 \cdot \omega \cdot S}{c^2} \cdot W = \frac{8 \cdot p \cdot n \cdot S}{c^2} \cdot W = \frac{8 \cdot p \cdot S}{l \cdot c} \quad (5)$$

where $\omega = 2 \cdot \pi \cdot \nu$, $l = \frac{C}{n}$.

Basic conditions of work of listed FOG not allow us to understand the constraints that are imposed on the accuracy of measurements made with it. Hitherto used fiber optic gyroscopes quartz fibers used in optical communications. In these fibers, that are amorphous, almost homogeneous and isotropic medium can propagate transverse optical waves. Light reflected from the interface "core-shell" as a result of total internal reflection propagates along the core as its own wave of the optical waveguide. Light wave as electromagnetic wave propagates along the fiber with a phase velocity is inversely proportional to the refractive index. Even a weak inhomogeneity can lead to cumulative effect and change the measurement result. Since the optical radiation propagates in a material medium, and it refers to the optical fiber, which is made of quartz or quartz glass, such physical phenomena as the birefringence effect, Kerr effect, Faraday effect, etc. adversely affect the angle of rotation loop fiber optic gyroscopes and registered phase of the optical signal. These effects associated with the process of optical radiation propagation in the material of the optical medium, leading to a phase shift of counter propagating waves, which is not associated with the rotation of the closed loop. The negative effects are also associated with the processes of scattering and reflection of light in an optical path, the polarization non-reciprocity effect associated with the asymmetric arrangement of anisotropic elements, relative to the centre of the fiber loop, or anisotropic fiber properties. However, the main problem of the FOG is that as the measuring accuracy and reducing the magnitude of the angular velocity measured is increasingly influenced by the optical effects not related to the angular displacement of the optical loop (FOG). Since the optical radiation propagates in a material medium, and it refers to the optical fiber, which is made of quartz or quartz glass, such physical phenomena as the birefringence effect, Kerr effect, Faraday effect, etc. adversely affect the angle of rotation loop fiber optic gyroscopes and registered phase of the optical signal. These effects associated with the process of optical radiation propagation in the material of the optical medium, leading to a phase shift of counter propagating waves, which is not associated with the rotation of the closed loop. The negative effects are also associated with the processes of scattering and reflec-

tion of light in an optical path, the polarization non-reciprocity effect associated with the asymmetric arrangement of anisotropic elements, relative to the centre of the fiber loop, or anisotropic fiber properties. This problem was solved, and solved by the use of frequency and phase modulation of the optical radiation is used, which allows to shift the zero point on the slope with the maximum slope of the interference signal. However, to get rid of the phase shifts, non-rotation circuit fails. Effects associated with locally mutual, non-stationary changes in the parameters of fiber, when they are excited asymmetrically with respect to the middle of the fiber loop. The main effects are the Faraday effect, Fresnel - Fizeau and nonlinear optical Kerr effect. The use of non-monochromatic radiation SLD (super luminescent diode with a coherence length of 10-20 microns) is practically eliminates the problem of the influence of the reflected and scattered radiation on the phase of the output signal of the FRI. However, the use of SLD removed only part of the problems leading to additional signals.

5. Photonic crystal fiber (PCF)

A photonic crystal fiber is an optical fiber which obtains its waveguide properties not from a spatially varying glass composition but from an arrangement of very tiny and closely spaced air holes which go through the whole length of fiber. Such air holes can be obtained by using a preform with (larger) holes, made e.g. by stacking capillary and/or solid tubes (stacked tube technique) and inserting them into a larger tube. Usually, this preform is then first drawn to a cane with a diameter of e.g. 1 mm, and thereafter into a fiber with the final diameter of e.g. 125 μm . Particularly soft glasses and polymers (plastics) also allow the fabrication of preforms for photonic crystal fibers by extrusion [4, 5]. There is a great variety of hole arrangements, leading to PCFs with very different properties. All these PCFs can be considered as specialty fibers. In this paper used the fibers of the type Hollow Core photonic crystal fiber, 1550 nm, $\text{Ø}10 \mu\text{m}$, core Hollow core Photonic Bandgap Fibers guide light in a hollow core, surrounded by a microstructured cladding of air holes and silica. Fig. 3 illustrated typical attenuation and dispersion.

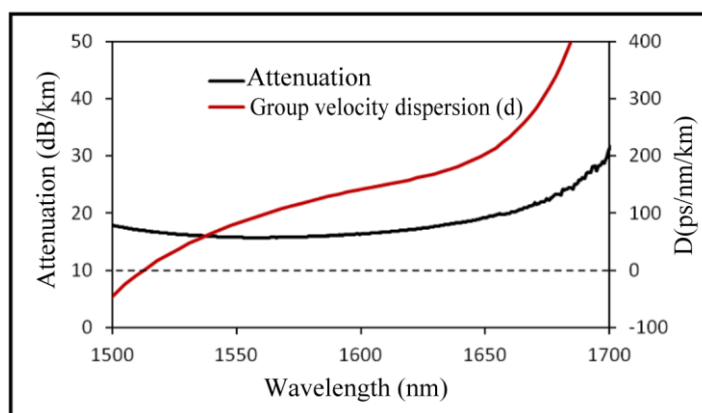


Fig. 3. Typical attenuation and dispersion

Since only a small fraction of the light propagates in silica, the effect of material nonlinearities is insignificant and the fibers do not suffer from the same limitations on loss as conventional fibers made from solid material alone.

6. Principles of operation of ring interferometer based on photonic crystal fibers

The main argument in favor of a replacement optical fiber to another medium, is that the first Sagnac experiments conducted in the hollow pipe and the low pressure air is not observed effects are manifested in the optical fiber. In this regard, it is evident that the use of such optical media, which on the one hand, would allow optical radiation to channel, and on the other hand did not change to its frequency and phase characteristics. Such environments include photonic crystals with defects. In such environments, the defect is a hollow waveguide. Manufactured photonic crystal fiber has a refractive index of 1.82 at wavelength 500 nm for this fiber type Kagome effective single-

mode propagation occurs in a wavelength range from 750 to 1050 nm in diameter mainly 30micron and loss of about 0.7 dB / m [6] see Fig. 4.

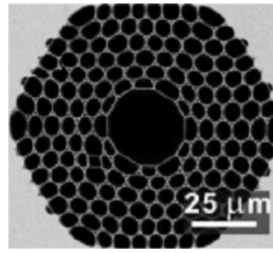


Fig. 4. An example of photonic crystal fiber with a hollow core diameter of about 30 microns

The collapsed zones in the PCF cause a broadening of the beam when it propagates from the SMF to the PCF [7, 8]. The broadening of the beam combined with the axial symmetry and the modal properties of the PCF are what allow the excitation (and recombination) of modes that have similar azimuthal symmetry [9]. The modes excited in the PCF have different effective indices (or different propagation constants), thus they travel at different speeds. As a result, the modes accumulate a phase difference as they propagate along the PCF. Due to the excitation and recombination of modes in the device, the reflection spectrum is expected to exhibit a series of maxima and minima (interference pattern). When two modes participate in the interference the transmitted or reflected intensity (I) can be expressed as:

$$I = I_1 + I_2 + 2\sqrt{I_1 I_2} \cos(Df) . \quad (6)$$

In Equation (6) I_1 and I_2 are, respectively, the intensity of the core mode and the cladding mode and $\Delta\Phi=2\pi\Delta nL/\lambda$ is the total phase shift. $\Delta n=n_f-n_c$, n_f and n_c being, respectively, the effective refractive index of the core mode and the cladding mode. L is the physical length of the PCF and λ the wavelength of the optical source. The fringe spacing or period (P) of the interference pattern is given by $P=\lambda^2/(\Delta nL)$. The maxima of the interference pattern appear at wavelengths that satisfy the condition $\Delta\Phi=2m\pi$, with $m=1, 2, 3 \dots$. This means at wavelengths given by

$$l_m = Dn \frac{L}{m} . \quad (7)$$

The fringe contrast or visibility (V) of a modal interferometer is an important parameter, particularly when the interferometer is used for sensing applications. Typically, higher visibility is desirable since it leads to larger signal-to-noise ratio and more accurate measurement. The visibility of a two-mode interferometer can be calculated by the well-known expression: $V=(I_{max}-I_{min})/(I_{max}+I_{min})$, where I_{max} and I_{min} are, respectively, the maximum and minimum values of I given in Equation (6). According to the definition and equation (6) V can be expressed as [10]:

$$V = \frac{2\sqrt{k}}{(1+k)} , \quad (8)$$

where $k=I_1/I_2$.

Many research groups prefer fringe contrast (expressed in dB) instead of visibility. The fringe contrast (FC) is defined here as $FC=-10\log(1-V)$. In Figure 5 we show the dependence of the fringe contrast on k along with the theoretical interference pattern of device with $L=10$ mm for two values of k . It can be noted that the fringe contrast increases as k approaches to 6, *i.e.*, when the two modes that participate in the interference have equal intensities (Fig. 5). Fringe contrast in a mode of interferometer as a function of k or the intensity of the cladding mode to that of the core mode ratio. The inset shows the theoretical reflection spectrum in the case of $k=0.4$ (dotted line) and $k=0.96$ (solid line).

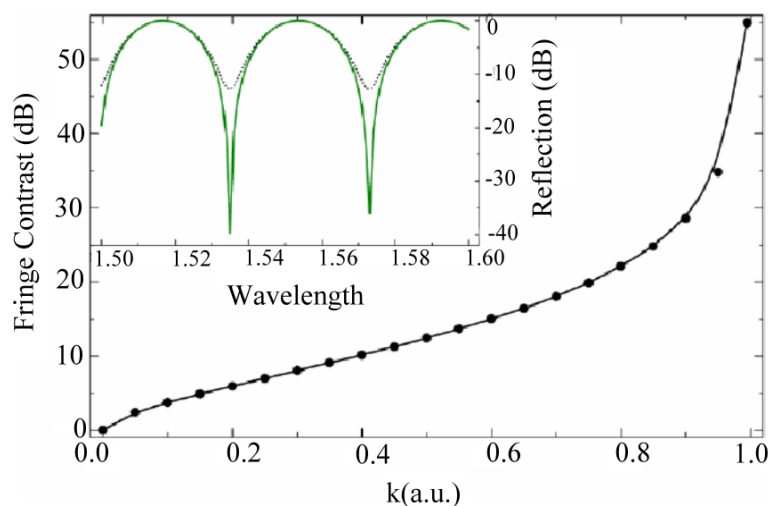


Fig. 5. Fringe contrast in a mode of interferometer

The physical mechanism for the waveguide propagation of radiation in photonic fibers is not associated with the phenomenon of total internal and with the presence of the photonic band gap in the transmission spectrum of the fiber cladding. Waveguides of this type are promising for the creation of gas sensors, spectral elements, as well as laser-cooled atoms management. Experimental studies have shown that in some cases [11] relatively high loss optical fibers with core air owing to scattering of light by irregularities of the glass surface due to the capillary waves frozen. Solution to reduce optical loss photonic fibers requires further fundamental research, however, we can already use small pieces of photonic fibers in special measuring instruments, which include the FOG. Photonic crystal fiber is a two-dimensional photonic crystal structure based on the song "quartz glass-to-air" formed in the shell.

7. Propagation of optical radiation in photonic crystal defect

In [12] were considered in detail the conditions of formation of photonic crystal fibers and spread them in the optical radiation. Experimental studies of PCF were conducted in a number of studies, for example, [13]. Photonic band gaps arising in the transmission spectrum of a two-dimensional periodic cladding, provides a high reflection coefficient for radiation propagating along the hollow core, realizing mode waveguide propagation. In [13] the results of an experimental determination of the optical emission intensity distribution in the cross-sectional center of the defect and the results of numerical calculation of the distribution of power density in cross-section are given. These results are shown in Fig. 6.

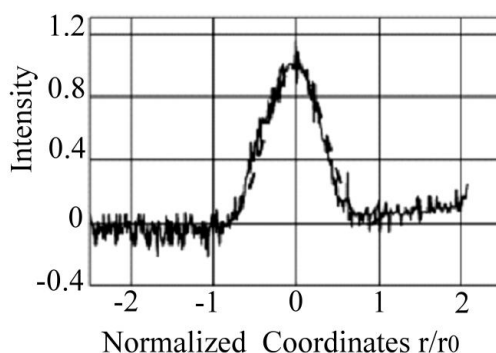


Fig. 6. Distribution of the output power with a hollow core PCF (solid line), numerical calculation of the intensity distribution (dashed line)

Fig. 7 illustrated the typical near field intensity profile.

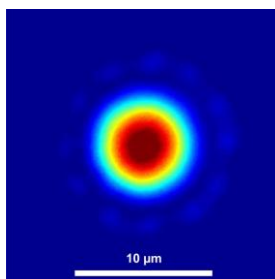


Fig. 7. Typical near field intensity profile

To date, published studies on the conditions of PCF usage for transmitting optical information signals in telecommunication systems, however, the use of PCF in optical interferometers have only begun to explore, for precision measurements of some physical quantities. In [14] the results of measurement of voltage using a cylindrical PCF, which is formed by the interferometer, are given. To describe the operation of a fiber gyroscope based on PCF must use the description of the optical waves propagating along the two-dimensional photonic crystal defect [15]. To implement the necessary PCF fiber gyroscope with a minimum loss of less than 1 dB / km, that extends single-mode radiation. These fibers include, for example, commercially available PCF - HC19-1550 (0,03 dB \ km) or LMA -25 (1,5 dB \ km) operating at 1550 nm. The low level of absorption in these fibers allows you to create on their basis multiturn ring interferometer, which implements the Sagnac effect. The main technical challenge in applying PCF is the junction of the individual elements of the PCF, Here are some distinctive features of the assembly fiber interferometer.

8. Technology development Opportunities

For hollow core fibers to realize their potential and advantages over conventional fibers in fiber optic gyroscopes, continued development is needed. Through its own internal development initiatives, and in collaboration with key customers and partners, these fibers have evolved and been used in early PCFG design evaluations and with positive results. Several areas for improvement that would help bring these fibers to the higher performance levels needed for practical implementation in commercial and military applications include:

8.1. Reduction of loss and backscatter

Long fiber lengths in a PCFG generally offer improved measurement sensitivity. The current loss levels of hollow core fibers designed for single mode transmission limit the fiber length. Although most of the light propagates in air, the portion that interacts with the silica hollow core wall experiences scattering and other loss mechanisms due to imperfections at this boundary. Advancements in design and processing techniques will be needed to improve these properties.

8.2. Redesign for smaller fiber geometry

The hollow core fibers described herein were designed with geometries for glass and coating diameter similar to conventional telecommunication fibers. For PCFG applications, coiling many turns of fiber benefits from a reduced diameter fiber, such as one with an 80 micron glass diameter, which is typical for many PCFGs. The hollow core fibers offer improved bend sensitivity allowing for tighter coils, but require a redesign of the fiber diameter to further reduce the space occupied by the fiber on the coil. This will require design and development activity to ensure that the reduced size will not compromise the optical performance produced by the special core and cladding bandgap regions.

8.3. Develop alternative termination and coupling options

Where the PCFG design can benefit from free space (air) coupling – such as in RFOG - the hollow core fiber offers a low reflectance interface, offering improved stability. Where designs require an alternative interface, such as a splice, mechanical coupling, or other type, reflections and

mechanical integrity of the interface will need to be managed. Development in this area would aim to provide termination and coupling options to provide the needed packaging and performance features for any particular design.

9. Conclusion

Due to their unique geometric structure, photonic crystal fibers present special properties and capabilities that lead to an outstanding potential for sensing applications. The report discusses the conditions of realization of the structure of the fiber gyroscope using a photonic crystal fiber. With this fiber, and methods and devices for forming fiber interferometers, can be solved the problem of creating a fiber-optic gyroscope based photonic - crystal fiber.

References: 1. *Fu, H.Y.* Pressure sensor realized with polarization-maintaining photonic crystal fiber-based Sagnac interferometer / H. Y. Fu, H. Y. Tam, L. Y. Shao, X. Dong, P. K. A. Wai, C. Lu, S. K. Khijwania // *Applied Optics*. – 2008. – Vol. 47. – P. 2835–2839. doi: 10.1364/ao.47.002835 . 2. *Andronova, I. A.* Physical problems of fibergiroscope based on the Sagnac effect / I. A. Andronova, G. B. Malykin // *Physics-Uspekhi*. – 2002. – Vol. 45, Issue 8. – P. 793–817. doi: 10.1070/pu2002v045n08abeh001073 . 3. *Shinde, Y. S. Gahir.* Dynamic pressure sensing study using photonic crystal fiber: application to tsunami sensing / Y. S. Shinde, H. K. Gahir // *IEEE Photonics Technology Letters*. – 2008. – Vol. 20, Issue 4. – P. 279–281. doi: 10.1109/lpt.2007.913741 . 4. *Ravi Kanth Kumar, V. V.* Extruded soft glass photonic crystal fiber for ultrabroad supercontinuum generation / V. V. Ravi Kanth Kumar, A. George, W. Reeves, J. Knight, P. Russell, F. Omenetto, A. Taylor // *Opt. Express*. – 2002. – Vol. 10, Issue 25. – P. 1520. doi: 10.1364/oe.10.001520 . 5. *Ebendorff-Heidepriem, H.* Suspended nanowires: fabrication, design and characterization of fibers with nanoscale cores / H. Ebendorff-Heidepriem, S. C. Warren-Smith, T. M. Monro // *Opt. Express*. – 2009. – Vol. 17, Issue 4. – P. 2646. doi: 10.1364/oe.17.002646 . 6. *Jiang, X.* Single-mode hollow-core photonic crystal fiber made from sift glass / X. Jiang, T. G. Euser, F. Abdolvand, F. Babic, F. Tani, N. Y. Joly, J. C. Travers, P. St. J. Russell // *Optics express*. – 2011. – Vol. 19, Issue 16. – P 15438–15444. doi: 10.1364/oe.19.015438 . 7. *Jha, R.* Ultrastable in reflection photonic crystal fiber modal interferometer for accurate refractive index sensing / R. Jha, J. Villatoro, G. Badenes // *Applied Physics Letters*. – 2008. – Vol. 93, Issue 19. – P. 191106:1–191106:3. doi: 10.1063/1.3025576 . 8. *Jha, R.* Refractometry based on a photonic crystal fiber interferometer / R. Jha, J. Villatoro, G. Badenes, V. Pruneri // *Optics Letters*. – 2009. – Vol. 34, Issue 5. – P. 617–619. doi: 10.1364/ol.34.000617 . 9. *Cárdenas-Sevilla, G. A.* Photonic crystal fiber sensor array based on modes overlapping / G. A. Cárdenas-Sevilla, V. Finazzi, J. Villatoro, V. Pruneri // *Optics Express*. – 2011. – Vol. 19, Issue 8. – P. 7596–7602. doi: 10.1364/oe.19.007596 . 10. *Zhang, Y.* Fringe visibility enhanced extrinsic Fabry-Perot interferometer using a graded index fiber collimator / Y. Zhang, Y. Li, T. Wei, X. Lan, Y. Huang, G. Chen, H. Xiao // *IEEE Photonics Journal*. – 2010. – Vol. 2, Issue 3. – P. 469–481. doi: 10.1109/jphot.2010.2049833 . 11. *Tuchin, V. V.* Sensornye svoystva fotonno-kristallicheskogo volnovoda s poloj serdcevinov / V. V. Tuchin, Ju. S. Skibina, V. I. Beloglazov et. al. // *Pis'ma v ZhTF*. – 2008. – Vol. 34, Issue 15. – P. 63–69. 12. *Russell, P. J.* Photonic-Cristal Fibers / P. J. Russell // *Journal of Lightwave technology*. – 2006. – Vol. 24, Issue 12. – P 4729–4749. 13. *Fedotov, A. B.* Volnovodnye svoystva i spektr sobstvennyh mod polyh fotonno-kristallicheskih volokon / A. B. Fedotov, S. O. Kononov, O. A. Koletovatova et. al. // *Kvantovaja jelektronika*. – 2003. – Vol. 33, Issue 3. – P. 271–274. 14. *Chen, W.* Ring-core photonic crystal fiber interferometer for strain measurement / W. Chen, S. Lou, L. Wang, S. Jian // *Optical Engineering*. – 2010. – Vol. 49, Issue 9. – P. 094402. doi: 10.1117/1.3488045 . 15. *Mogilevtsev, D.* Localized Function Method for Modelling Defect Modes in 2-d Photonic Cristals / D. Mogilevtsev, T. A. Birks, P. J. Russell // *Journal of lightwave technology*. – 1999. – Vol. 17, Issue 11. – P. 2078–2081. doi: 0.1109/50.802997

Харьковский национальный
университет радиоэлектроники

Поступила в редколлегию 17.02.2015